

Single-Molecule Experiments in Synthetic Biology: An Approach to the Affinity Ranking of DNA-Binding Peptides**

Rainer Eckel, Sven David Wilking, Anke Becker,
Norbert Sewald,* Robert Ros, and Dario Anselmetti*

Gene expression in eukaryotes is controlled at the transcriptional level by the specific binding of transcription factors to defined DNA sequences. In this way, cell growth, differentiation, and development are regulated. The possibility to influence and control cell metabolism through modified synthetic transcription factors^[1–4] offers fascinating prospects for molecular cell biology in the framework of biomimetics and synthetic biology.^[5,6] The design and synthesis of biologically active artificial enzymes and new protein-based materials can be investigated by the combination of bioorganic bottom-up synthesis and single-molecule affinity nanotechnology. With this approach important questions can be addressed, such as the extent to which a single recognition helix contributes to the specific binding of a complete protein

to DNA, the effect that a single amino acid point mutation has upon biological specificity and affinity, and the minimal peptide sequence length to ensure binding specificity. This approach would also aid in the design of artificial proteins that contain a purely synthetic helix-turn-helix (HTH) binding motif.

In this context, it is of considerable interest to elucidate the DNA-binding specificity of synthetic peptides with a primary sequence akin to the binding domain of a transcription factor. We studied a 20-residue peptide that represents the native sequence of a binding epitope of the transcription activator PhoB (*E. coli*) and three single point mutants of this peptide.

PhoB is a transcription activator which, after phosphorylation by PhoR, binds to the phosphate box in the promoter region of the phosphate regulon *pho* and activates the expression of genes involved in phosphate metabolism.^[7–9] The protein^[9] consists of a regulatory phosphorylation domain in the N-terminal region (PhoB 1–127) and a DNA-binding domain in the C-terminal region (PhoB 128–229). Deletion experiments showed that PhoB 139–229 binds to double-stranded DNA and recognizes the sequence TGTCA. The NMR solution structure of the regulatory domain and the DNA-binding domain (PhoB126–229),^[10] as well as the X-ray crystal structure of the complex with DNA have been reported (Figure 1a).^[11] Structurally, the DNA-binding domain of PhoB belongs to the family of *winged* helix-turn-helix proteins with the topology β^1 - β^2 - β^3 - β^4 - α^1 - β^5 - α^2 - α^3 - β^6 - β^7 , in which the rigid turn is replaced by a loop. This family is characterized by an N-terminal four-stranded β sheet (β^1 - β^2 - β^3 - β^4), one α helix (α^1) connected through a short β sheet (β^5) to another α helix (α^2), followed by a third α helix (α^3) and a β hairpin (β^6 - β^7). The DNA-recognizing helix α^3 , is amphiphilic and is connected to α^2 by a loop.^[12] The β hairpin (β^6 -turn- β^7) is often called the *recognition wing*.^[13]

The single amino acid residues of DNA-binding peptides and proteins contribute differently to affinity and specificity. Whereas cationic side chains (Lys, Arg) often form sequence-independent ionic interactions with the phosphate backbone, the sequence information of the DNA is read through hydrogen bonds and van der Waals interactions with the peptide. Binding of the recognition helix α^3 of PhoB takes place in the DNA major groove.^[11] Arg201 interacts through a hydrogen bond with the carbonyl oxygen atom of a guanine base while Arg193, His198, Arg200, and Arg203 form salt bridges with phosphate groups. Furthermore, van der Waals contacts with Thr194 and Val197 are involved in specific recognition. Arg219 in the *recognition wing* is bound to deoxyribose moieties through hydrogen bonds.

In the work reported herein, the contribution that single amino acid residues in the DNA-binding helix α^3 contribute to intermolecular affinity was investigated on the single-molecule level. We synthesized peptides in which the amino acid residues that interact with the DNA phosphate backbone in the X-ray crystal structure through salt bridges were individually exchanged by alanine (Table 1). The synthesized peptides comprised the native sequence PhoB(190–209) as well as the point-mutated peptides PhoB(190–209) R193A, PhoB(190–209) H198A and PhoB(190–209) R203A. Accord-

[*] Dipl.-Chem. R. Eckel, Priv.-Doz. Dr. R. Ros, Prof. Dr. D. Anselmetti
Experimental Biophysics and Applied Nanoscience
Bielefeld University
Universitätsstraße 25, 33615 Bielefeld (Germany)
Fax: (+49) 521-106-2959
E-mail: dario.anselmetti@physik.uni-bielefeld.de
Dipl.-Chem. S. D. Wilking, Prof. Dr. N. Sewald
Organic and Bioorganic Chemistry
Bielefeld University
Universitätsstraße 25, 33615 Bielefeld (Germany)
Fax: (+49) 521-106-8094
E-mail: norbert.sewald@uni-bielefeld.de
Priv.-Doz. Dr. A. Becker
Genetics
Bielefeld University (Germany)

[**] The authors thank the Deutsche Forschungsgemeinschaft (SFB 613) for financial support, Tanja Beschnitt for help with DNA preparation, and Kay Lofthouse for a careful reading of the manuscript.

Supporting information for this article is available on the WWW under <http://www.angewandte.org> or from the author.

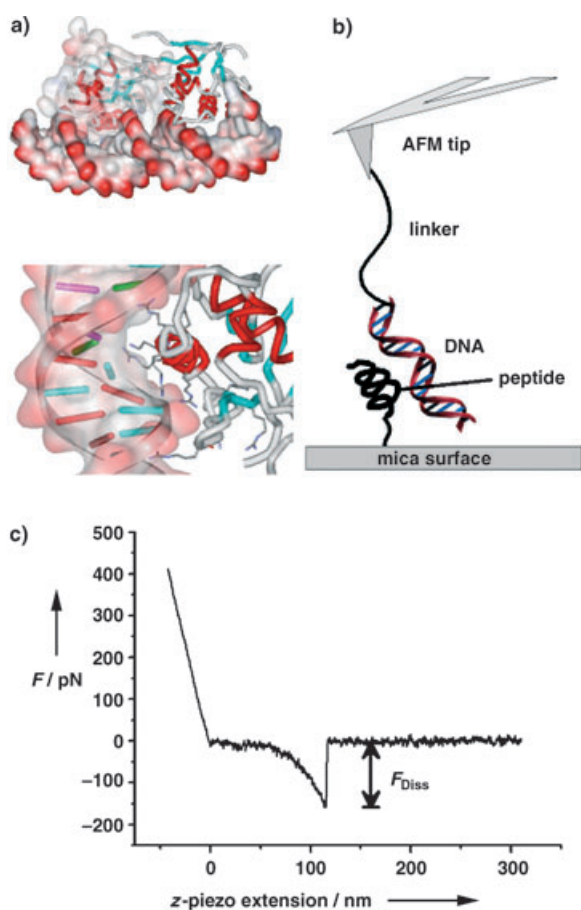


Figure 1. a) Upper image: X-ray crystal structure of the 2:1 complex of PhoB(124–229) with DNA,^[10] lower image: Section from the X-ray crystal structure showing the recognition helix α^3 ; b) force spectroscopy setup (schematic representation); c) typical force–distance curve (only retractive part shown).

Table 1: Synthesized peptides from the epitope PhoB(190–209).

Mutation	Peptide Sequence	$k_{\text{off}} [\text{s}^{-1}]^{\text{[a]}}$	$x_{\beta} [\text{\AA}]^{\text{[a]}}$
–	Ac-VEDRTVDVHIRRLRKALEPG-Linker	3.1 ± 2.1	6.8 ± 1.2
R193A	Ac-VED A TVDVHIRRLRKALEPG-Linker	0.071 ± 0.053	9.3 ± 2.6
H198A	Ac-VEDRTVDV A IRRLRKALEPG-Linker	49.5 ± 21.2	7.2 ± 3.5
R203A	Ac-VEDRTVDVHIRRL A KALEPG-Linker	no binding	no binding

[a] k_{off} : dissociation rate constant for the peptide–DNA complex; x_{β} : molecular reaction length.

ing to CD spectroscopy measurements, all peptides exhibit an α -helical structure. N-terminal functionalized fragments of the PhoB helix α^3 were synthesized on the solid phase with 2-chlorotritylresin preloaded with a suitable linker according to the Fmoc/tBu protection scheme.^[14] The peptides were purified by HPLC with acetonitrile/water/TFA gradients. The interaction of the synthesized peptides with the corresponding DNA was investigated with AFM force spectroscopy.

A broad affinity range for specific molecular recognition between single binding partners from $10^{-5} \text{ M}^{\text{[15]}}$ to $10^{-15} \text{ M}^{\text{[16,17]}}$ can be investigated with single-molecule force spectroscopy. The deflection of a micro-fabricated force sensor (cantilever) is used to detect forces in the piconewton range. The AFM

principle permits investigation of molecular binding forces under physiological conditions, and AFM force spectroscopy has found applications in the study of a variety of specific biological receptor–ligand interactions^[16–22] as well as in supramolecular host–guest systems.^[15] The direct investigation of specific, native protein–DNA interactions has been reported recently.^[23–25]

In our studies reported herein, we applied AFM single-molecule force spectroscopy to study the specific binding between the peptides listed in Table 1 and the DNA target sequence. Each peptide was covalently immobilized to an amino-functionalized mica surface in a directed manner with the short C-terminal linker 1,8-diamino-3,6-dioxaoctane and the cross-linker BS³ (bis(sulfosuccinimidyl)suberate; Figure 1b). This immobilization prevents unfolding of the peptide caused by physisorption on the surface. PCR-amplified genomic DNA containing the 600-bp PhoB binding motif from *E. coli* was chosen as the binding partner, and was bound to an AFM tip with a bifunctional polyethylene glycol (PEG) linker (molar mass: 3400 g mol^{-1} , corresponding to an average length of 30 nm).^[26] The application of the PEG linker serves various purposes. First, it adds steric flexibility to the system and ensures that dissociation occurs far from the surface. Second, the linker facilitates the distinction between single and multiple dissociation events, and decreases non-specific adhesion. Third, the elastic stretching of the linker ensures a gradual increase in force until the point of bond rupture, and allows precise measurement of the molecular elasticity of the complex (Figure 1c). As the elasticity is determined for each rupture event individually, variations in the entropic portion of the rupture peaks are included and do not affect the statistical interpretation.

Compilation of the rupture forces to histograms and statistical analysis of the resulting force distribution yields the most probable dissociation forces at a given retract velocity. Each histogram represents the analysis of 2000 force curves; the binding probabilities given in the figures (Figure 2 and Supporting Information) refer to the ratio of rupture events divided by the total number of force curves recorded (for example, 300 binding events out of 2000 force curves results in a binding probability of 15%). The maximum of the force distribution was taken as the most probable dissociation force.

Competition experiments were performed to determine if binding between the peptides and the DNA target sequence occurs specifically. For each mutant, a series of force spectroscopy experiments in standard buffer solution ($100 \text{ mM Na}_2\text{HPO}_4$, 50 mM NaCl , pH 7.4) was followed by a series of experiments with an excess of free binding partner (peptide or DNA) as competitor in solution. This was followed by washing the sample with standard buffer and then performing another series of experiments in standard buffer. Figure 2 shows the results of the competition for the native peptide: part (a) shows the force distribution in standard buffer solution, with a total binding probability of $\approx 33\%$; part (b) shows the competition with free peptide in

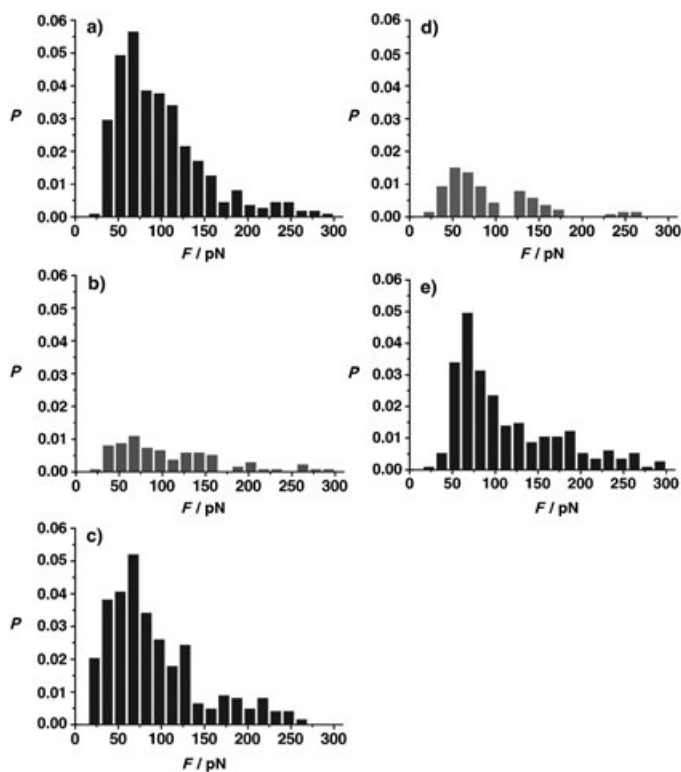


Figure 2. Competition experiments with the native peptide sequence: a) force spectroscopy experiment in standard buffer solution (100 mM NaH_2PO_4 , 50 mM NaCl, pH 7.4) without competitor; b) experiment in buffer solution with an excess of free peptide as competitor; c) experiment after washing with standard buffer solution; d) experiment in buffer solution with excess of free DNA as competitor; e) as in c).

buffer solution, in which a significant decrease in total binding probability is apparent; part (c) illustrates how the original binding probability and activity of the interaction is restored after washing the sample in standard buffer; part (d) shows the analogous competition experiment with excess free DNA in buffer solution, and part (e) illustrates the reactivation of the interaction. In additional control experiments with EBNA DNA fragments, which lack the PhoB binding sequence, no binding was observed at all (data not shown; EBNA = Epstein–Barr virus nuclear antigen). These results clearly prove that the binding of the peptide with the native sequence takes place specifically at the binding sequence on the DNA.

The same conclusion applies to the results of the competition experiments performed with the peptide mutants R193A and H198A. Again, competition was successful both with free peptide and with free DNA as competitor (Supporting Information). For H198A, however, the total binding probability was distinctly lower than those of the native peptide and the mutant R193A. In contrast, binding experiments with the mutant R203A yielded very few binding events, rendering statistical analysis impossible. In summary, there is evidence that the native sequence and the mutants R193A and H198A specifically recognize the PhoB target sequence. As it was doubted recently that short peptide sequences with only one α helix are capable of specific DNA binding,^[1] our results are quite remarkable given that the 20-

residue peptides represent a rather small epitope from the binding domain of the protein.

Dynamic force spectroscopy experiments were performed with the native sequence and the mutants R193A and H198A to obtain information on the dissociation kinetics and energy landscapes. In force-induced thermally driven dissociation of a metastable molecular complex,^[27–29] the measured dissociation forces depend on the temporal force evolution on the complex, commonly referred to as the loading rate. It is given as the product of the molecular elasticity and the retract velocity of the cantilever. In our experiments, the molecular elasticity was determined by fitting the last 20 data points prior to bond rupture in the force–distance curve. The retract velocity was varied in the range of 10–6000 nm s^{-1} .

The results of the dynamic experiments are shown in Figure 3. The dissociation forces (derived from analysis of the

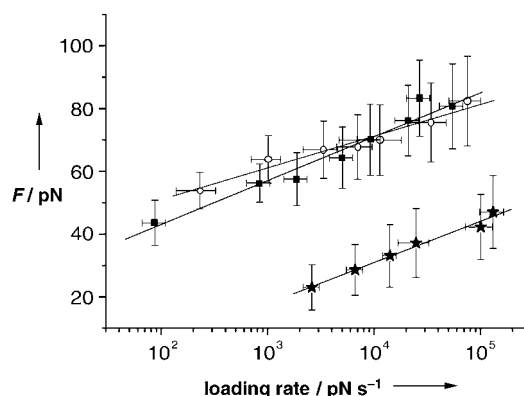


Figure 3. Dynamic force spectroscopy: ■ = native sequence; ○ = R193A; * = H198A.

respective force histograms) are plotted logarithmically against the loading rate. The linear fit of the data provides two important parameters. First, extrapolation to zero external force $F=0$ gives the thermal off-rate k_{off} . For the native sequence, the thermal off-rate amounts to $k_{\text{off}} = (3.1 \pm 2.1) \text{ s}^{-1}$ (Table 1), which corresponds to a time constant (lifetime) for complex dissociation of $\tau = (320 \pm 220) \text{ ms}$. The complex between DNA and the mutant R193A, interestingly, dissociates more slowly, with $k_{\text{off}} = (0.071 \pm 0.053) \text{ s}^{-1}$, indicating a longer complex lifetime of $\tau = (14.1 \pm 10.5) \text{ s}$. In contrast, the mutant H198A exhibits a considerably higher off-rate: $k_{\text{off}} = (49.5 \pm 21.2) \text{ s}^{-1}$, corresponding to a shorter lifetime of $\tau = (20 \pm 8) \text{ ms}$. This is not surprising, as in mutant H198A the basic residue His 198 from the native sequence was replaced by alanine. Hence, the charge-controlled contribution to the binding of the peptide with DNA should be decreased. Surprisingly, the mutant R193A, in which Arg 193 was replaced by an alanine, exhibits a lower off-rate and consequently, a longer complex lifetime than the native peptide sequence. This result can presumably be attributed to an enhanced α -helical conformation of the peptide in solution, a finding which will be examined more closely in future experiments. In comparison with recent single-molecule experiments with complete transcription-activating proteins bearing a HTH DNA-binding motif,

which exhibit lower dissociation rates (2×10^{-4} to $1.3 \times 10^{-2} \text{ s}^{-1}$)^[23] and lifetimes (100–1000 s), this interesting fact indicates the presence and importance of cooperative binding effects—an issue which must be addressed in the future as well.

The affinity of a ligand to its receptor, represented in the case of a 1:1 kinetics by the dissociation equilibrium constant $K_D = k_{\text{off}}/k_{\text{on}}$, is governed by the dissociation rate k_{off} .^[22] Assuming diffusion-controlled association with a typical on-rate constant of $k_{\text{on}} = 10^5 \text{ M}^{-1} \text{ s}^{-1}$ ^[24,30–32] for the binding of a peptide to the target DNA, equilibrium constants of $K_D = 3 \times 10^{-6} \text{ M}$ (native sequence), $K_D = 7 \times 10^{-8} \text{ M}$ (mutant R193A), and $K_D = 5 \times 10^{-5} \text{ M}$ (mutant H198A) can be estimated. According to $\Delta G^\circ = RT \ln K_D$, the corresponding Gibbs' free energy differences of complex formation can be estimated to $\Delta G^\circ = -31 \text{ kJ mol}^{-1}$ (native sequence), $\Delta G^\circ = -41 \text{ kJ mol}^{-1}$ (mutant R193A), and $\Delta G^\circ = -25 \text{ kJ mol}^{-1}$ (mutant H198A).

From the inverse slope of the linear fit to the data (Figure 3), a molecular reaction length x_β can be obtained as a second parameter, which amounts to values of $6.8 \pm 1.2 \text{ \AA}$ for the native peptide and $7.2 \pm 3.5 \text{ \AA}$ for the mutant H198A (Table 1). However, for peptide R193A, which exhibits the longest complex lifetime, a larger value of $x_\beta = 9.3 \pm 2.6 \text{ \AA}$ is found. This is consistent with the previous results, as it indicates that the final activation barrier is located late along the reaction coordinate. This suggests the possibility for the complex to re-associate (assuming microscopic reversibility) over a larger distance along the reaction coordinate, which corresponds to a longer lifetime of the complex.

In summary, the specific interaction of synthetic peptides that comprise only the recognition helix of a transcription activator with DNA could be investigated for the first time at the single-molecule level. The molecular binding forces observed for single peptide–DNA complexes upon induced dissociation were analyzed quantitatively with AFM force spectroscopy. Competition experiments have proven the specific binding of two peptide mutants to DNA. The results of dynamic force spectroscopy experiments indicate a dependence of the binding forces on external load, which is consistent with thermally driven dissociation. These experiments yield values for the dissociation rates of the corresponding complexes, which allow a direct affinity ranking of synthetic peptides with single point mutations. Furthermore, our results indicate the importance of peptide length, cooperative binding effects, and the contribution of single point mutations to the specific binding of (synthetic) peptides to DNA. These results prove the potential of combining chemical synthesis strategies for biomimetics (synthetic biology) with the high sensitivity of AFM single-molecule force spectroscopy to investigate, quantify, and control the mechanisms and properties of molecular recognition processes (molecular nanotechnology).

Received: January 14, 2005

Revised: March 3, 2005

Published online: May 20, 2005

Keywords: molecular recognition · peptides · point mutations · scanning probe microscopy · single-molecule studies

- [1] M. E. Vázquez, A. M. Caamaño, J. L. Mascarenas, *Chem. Soc. Rev.* **2003**, 32, 338–349.
- [2] M. E. Vázquez, A. M. Caamaño, J. Martínez-Costas, L. Castedo, J. L. Mascarenas, *Angew. Chem.* **2001**, 113, 4859–4861; *Angew. Chem. Int. Ed.* **2001**, 40, 4723–4725.
- [3] A. M. Caamaño, M. E. Vázquez, J. Martínez-Costas, L. Castedo, J. L. Mascarenas, *Angew. Chem.* **2000**, 112, 3234–3237; *Angew. Chem. Int. Ed.* **2000**, 39, 3104–3107.
- [4] C. Melander, R. Burnett, J. M. Gottesfeld, *J. Biotechnol.* **2004**, 112, 195–220.
- [5] P. Ball, *Nanotechnology* **2005**, 16, R1–R8.
- [6] S. A. Benner, *Nature* **2003**, 421, 118–118.
- [7] S.-K. Kim, S. Kimura, H. Shinagawa, A. Nakata, K.-S. Lee, B. L. Wanner, K. Makino, *J. Bacteriol.* **2000**, 182, 5596–5599.
- [8] K. Makino, H. Shinagawa, M. Amemura, A. Nakata, *J. Mol. Biol.* **1986**, 190, 37–44.
- [9] K. Makino, M. Amemura, T. Kawamoto, K. Kimura, H. Shinagawa, A. Nakata, M. Suzuki, *J. Mol. Biol.* **1996**, 259, 15–26.
- [10] Brookhaven Data Base: 1QQI. 2004.
- [11] A. G. Blanco, M. Sola, F. X. Gomis-Rüth, M. Coll, *Structure* **2002**, 10, 701–713.
- [12] H. Okamura, S. Hanaoka, A. Nagadoi, K. Makino, Y. Nishimura, *J. Mol. Biol.* **2000**, 295, 1225–1236.
- [13] E. Martínez-Hackert, A. M. Stock, *J. Mol. Biol.* **1997**, 269, 301–312.
- [14] S. D. Wilking, N. Sewald, *J. Biotechnol.* **2004**, 112, 109–114.
- [15] R. Eckel, R. Ros, B. Decker, J. Mattay, D. Anselmetti, *Angew. Chem.* **2005**, 117, 489–492; *Angew. Chem. Int. Ed.* **2005**, 44, 484–488.
- [16] E.-L. Florin, V. T. Moy, H. E. Gaub, *Science* **1994**, 264, 415–417.
- [17] G. U. Lee, D. A. Kidwell, R. J. Colton, *Langmuir* **1994**, 10, 354–357.
- [18] U. Dammer, O. Popescu, P. Wagner, D. Anselmetti, H.-J. Güntherodt, G. N. Misevic, *Science* **1995**, 267, 1173–1175.
- [19] T. Strunz, K. Oroszlan, R. Schäfer, H.-J. Güntherodt, *Proc. Natl. Acad. Sci. USA* **1999**, 96, 11277–11282.
- [20] R. Ros, F. Schwesinger, D. Anselmetti, M. Kubon, R. Schäfer, A. Plückthun, L. Tiefenauer, *Proc. Natl. Acad. Sci. USA* **1998**, 95, 7402–7405.
- [21] U. Dammer, M. Hegner, D. Anselmetti, P. Wagner, M. Dreier, W. Huber, H.-J. Güntherodt, *Biophys. J.* **1996**, 70, 2437–2441.
- [22] F. Schwesinger, R. Ros, T. Strunz, D. Anselmetti, H.-J. Güntherodt, A. Honegger, L. Jeremus, L. Tiefenauer, A. Plückthun, *Proc. Natl. Acad. Sci. USA* **2000**, 97, 9972–9977.
- [23] F. W. Bartels, B. Baumgarth, D. Anselmetti, R. Ros, A. Becker, *J. Struct. Biol.* **2003**, 143, 145–152.
- [24] B. Baumgarth, F. W. Bartels, D. Anselmetti, A. Becker, R. Ros, *Microbiology* **2005**, 151, 259–268.
- [25] F. Kühner, L. T. Costa, P. M. Bisch, S. Thalhammer, W. M. Heckl, H. E. Gaub, *Biophys. J.* **2004**, 87, 2683–2690.
- [26] P. Hinterdorfer, W. Baumgartner, H. Gruber, K. Schilcher, H. Schindler, *Proc. Natl. Acad. Sci. USA* **1996**, 93, 3477–3481.
- [27] G. I. Bell, *Science* **1978**, 200, 618–627.
- [28] E. Evans, K. Ritchie, *Biophys. J.* **1997**, 72, 1541–1555.
- [29] R. Merkel, P. Nassoy, A. Leung, K. Ritchie, E. Evans, *Nature* **1999**, 397, 50–53.
- [30] M. Schlosshauer, D. Baker, *Protein Sci.* **2004**, 13, 1660–1669.
- [31] M. Vijayakumar, K.-W. Wong, G. Schreiber, A. R. Fersht, A. Szabo, H.-X. Zhou, *J. Mol. Biol.* **1998**, 278, 1015–1024.
- [32] O. G. Berg, R. B. Winter, P. H. von Hippel, *Biochemistry* **1981**, 20, 6929–6948.